

Polynomial Eulerian shape distributions

Francisco J. Caro-Lopera *

Departament of Basic Sciences
 Universidad de Medellín
 Medellín, Colombia
 E-mail: fcaro@udem.edu.co

José A. Díaz-García

Universidad Autónoma Agraria Antonio Narro
 Calzada Antonio Narro 1923, Col. Buenavista
 25315 Saltillo, Coahuila, México
 E-mail: jadiaz@uaaan.mx

Abstract

In this paper a new approach is derived in the context of shape theory. The implemented methodology is motivated in an open problem proposed in Goodall and Mardia (1993) about the construction of certain shape density involving Euler hypergeometric functions of matrix arguments.

The associated distribution is obtained by establishing a connection between the required shape invariants and a known result on squared canonical correlations available since 1963; as usual in statistical shape theory and the addressed result, the densities are expressed in terms of infinite series of zonal polynomials which involves considerable difficulties in inference. Then the work proceeds to solve analytically the problem of computation by using the Eulerian matrix relation of two matrix argument for deriving the corresponding polynomial distribution in certain parametric space which allows to perform exact inference based on exact distributions characterized for polynomials of very low degree. A methodology for comparing correlation shape structure is proposed and applied in handwritten differentiation.

1 Introduction

Invariant statistics has emerged as one of the most powerful tools in statistics to study matrix variate problems, in particular the statistical shape analysis has been rolled a number of applications in almost all the natural and exact sciences; their applications in machine vision and images analysis are notable. In general, shape theory deals with problems of differentiation of “objects” which can be summarized by anatomical or mathematical marks called landmarks, under the assumption that those points can be placed (in presence of randomness) in any similar objects and absorbs all the geometrical information of the “shape”

*Corresponding author

Key words. Euler matrix relation, zonal polynomials, shape theory, correlation structure, polynomial distributions.

2000 Mathematical Subject Classification. 15A23; 15B33; 15A09; 15B52; 60E05

of the object. The invariant theory enters in the analysis, when the comparisons, matching, and/or inference are performed in special quotient spaces rather than the usual full noised Euclidean space. Then according to the symmetries involved in the study defined and supervised by the expert in the experiment, a number of different shapes can be defined. Three classical shapes are well studied in literature, the Euclidean or similarity shape, the affine or configuration, and the projective shape; then the associated shape is all geometrical information which remains under removing location, rotation, scaling, reflection, uniform shear and/or projection, etc., see for example, Dryden and Mardia (1998) and the references therein.

Under deterministic assumptions, shape theory counts a number of approaches, a source of their main aspects are given for example in Kendall *et al.* (1999), their references; as a consequence of this geometrical understanding of shape, the procrustes theory, including projective shape analysis and its relation to affine shape analysis, have been studied profusely in applications; some works in these directions are due to Mardia *et al.* (2005), Patrangenaru and Mardia (2003), Mai *et al.* (2011), Domokos and Kato (2010), Ecaberth and Thiran (2004), Glasbey and Mardia (2001), Goodall (1991), Groisser and Tagare (2009), Lindeberg and Garding (1997), Mardia *et al.* (1996), Mardia and Patrangenaru (2005), Mokhtarian and Abbasi (2002), Horgan *et al.* (1992), Kent *et al.* (2004), Lin and Fang (2007), among many others

Now, the statistical theory of shape deals with landmarks in presence of random (see for example Dryden and Mardia (1998), Small (1996) and the references therein). A branch of the statistical shape analysis was connected by Goodall and Mardia (1993)(corrected by Díaz-García *et al.* (2003) and Caro-Lopera *et al.* (2010))) with the very old theory of matrix variate distribution based on A.T. James zonal polynomials (see for example James (1964) and the cited papers). At that time the shape distributions derived in Goodall and Mardia (1993) and most of the classical results in matrix variate distributions collected in the excellent book of Muirhead (1982) could not be computed and forced to use asymptotic distributions. Only recently the zonal polynomials were computable in an efficient way by Koev and Edelman (2006), and a hope for computations of infinite series of zonal polynomials was a possible task under certain restriction and subject to the problem of automatic detection of convergence of the series.

Parallel to the problem of computation, the classical shape theory of Goodall and Mardia (1993) based on the Gaussian distributions, opened a field of new interesting theoretical and applied problems, the so called generalized shape theory, which models shape under non Gaussian models, see for example, Caro-Lopera *et al.* (2009b, 2010); Caro-Lopera *et al.* (2014c), Díaz-García & Caro-Lopera (2012a,b, 2014); Díaz-García and Caro-Lopera (2016) and Caro-Lopera *et al.* (2013a), among many others. Moreover the generalized shape analysis can be studied in the more general setting of real normed division algebras, a unified approach valid for real, complex, quaternion and octonion landmark data matrices Díaz-García & Caro-Lopera (2010).

As it can be checked in the above references the Euclidean shape based on similarity transformations, in all their forms, and the affine configuration have been studied extensively, involving inference, families of distributions and so on; however, an open problem seems to be unsolved from the times of Goodall and Mardia (1993).

Analysis of shape under Gaussian models were proposed by Goodall and Mardia (1993) following a natural induction way of deriving new shape distribution via Laplace-transform in order to obtain hypergeometric series of matrix arguments by known integration over cones and manifolds involving zonal polynomials. This methodology was thought for obtaining successive distributions which filter new more valuable information of the original landmark data.

The underlying sequence of new shape distributions appeared as follows: start with an

original Gaussian landmark data, then after removing traslation and rotation the so called size and shape distribution is obtained, this function has the form of a ${}_0F_1(\cdot)$ hypergeometric function Bessel type (see Muirhead (1982)), a known series of zonal polynomials. According to the inductive process of constructing hypergeometric series, the next appropriate shape should be a confluent type ${}_1F_1(\cdot)$ by removing the scaling information of the size and shape, then the shape distribution is gotten. But as it can be seen in Goodall and Mardia (1993), this shape has not the required form and no properties were available at that time to explore the asymptotics or computation of the distribution (later Díaz-García & Caro-Lopera (2012a,b, 2014); Díaz-García and Caro-Lopera (2016) generalized the result to every elliptical model and transformations and performed inference with the exact densities). So, in order to obtain confluent shape distribution, Goodall and Mardia (1993) defined an affine transformation which lead directly from the Helmertized matrix (the original Gaussian landmark matrix invariant under traslation) to the required confluent distribution (later Caro-Lopera *et al.* (2009b, 2010); Caro-Lopera *et al.* (2014c) generalized it to the class of elliptical distribution and performed inference with the exact distribution, some of them simple polynomials of low degree). Finally, Goodall and Mardia (1993) conjectured that a new class of shape distributions could be constructed by using the induction way and claimed for an hypergeometric type shape distribution ${}_2F_1(\cdot)$.

In this paper we study the addressed open problem by defining a new approach in the context of statistical shape theory. Section 2 focus in the definition of the new shape invariant. As very usual in shape theory, the resulting density is a series of zonal polynomials which presents strong problems for inference; it motivated Section 3 which solves the problem of inference by considering in some simple parametric space an equivalent polynomial distribution of very low degree in the latent roots of the matrix arguments of the zonal polynomials, then the exact formulae available for these polynomials in two dimensions, a number of applications and methodologies for shape comparisons are given in Section 4.

2 Eulerian Shape

The aim of this approach consists of proposing an alternative way to compare populations in the context of the shape theory. It is easy to check in the literature shape that Wilks' theorem is the most common resource for testing means of two populations (a number of other tests can be implemented, see Díaz-García and Caro-Lopera (2008)), Caro-Lopera *et al.* (2010,?). However, the application of the classical chi-squared distribution of that theorem demands a number of conditions on regularity which are difficult to keep in most of the available landmark data.

The strength of relation between two variates has a similar power of explanation in shape theory than the equality of means and both complement each other for completing a shape analysis.

Consider two $N \times K$ matrices \mathbf{X}^{**} and \mathbf{Y}^{**} , which summarize two figures comprised in N landmarks in K dimensions, such that $\mathbf{X}^{**} \sim \mathcal{N}(\boldsymbol{\mu}_{\mathbf{X}^{**}}, \mathbf{I}_N \otimes \boldsymbol{\Phi}_{\mathbf{X}^{**}})$ and $\mathbf{Y}^{**} \sim \mathcal{N}(\boldsymbol{\mu}_{\mathbf{Y}^{**}}, \mathbf{I}_N \otimes \boldsymbol{\Phi}_{\mathbf{Y}^{**}})$, where $\boldsymbol{\Phi}_{\mathbf{X}^{**}}$ and $\boldsymbol{\Phi}_{\mathbf{Y}^{**}}$ are positive definite $K \times K$ matrices.

Now, as usual in shape theory we remove some meaningless geometrical information as the translation of both figures, by using contrast matrices, for example sub-Helmert arrays. In this case we use a $(N - 1) \times N$ matrix, \mathbf{L} , which has orthonormal rows to $\mathbf{1} = (1, \dots, 1)'$; to construct the so called Helmertized $N - 1 \times K$ matrices, say, \mathbf{X}^* and \mathbf{Y}^* , respectively, via $\mathbf{LX}^{**} = \mathbf{X}^*$ and $\mathbf{LY}^{**} = \mathbf{Y}^*$.

Under these transformations, the randomness of the transformed landmarks follow the laws: $\mathbf{X}^* \sim \mathcal{N}(\boldsymbol{\mu}_{\mathbf{X}^*}, \mathbf{I}_n \otimes \boldsymbol{\Sigma}_{22})$, $\mathbf{Y}^* \sim \mathcal{N}(\boldsymbol{\mu}_{\mathbf{Y}^*}, \mathbf{I}_n \otimes \boldsymbol{\Sigma}_{11})$, where $n = N - 1 \times K$. The means are changed to $\boldsymbol{\mu}_{\mathbf{X}^*} = \mathbf{L}\boldsymbol{\mu}_{\mathbf{X}^{**}}$ and $\boldsymbol{\mu}_{\mathbf{Y}^*} = \mathbf{L}\boldsymbol{\mu}_{\mathbf{Y}^{**}}$, while the new covariance matrices are

conveniently denoted by Σ_{11} and Σ_{22} , where $\Sigma_{11} = \mathbf{L}\Phi_{\mathbf{Y}^{**}}\mathbf{L}'$ and $\Sigma_{22} = \mathbf{L}\Phi_{\mathbf{X}^{**}}\mathbf{L}'$.

We storage the above Helmertized matrices into an $N \times 2K$ partition array $\mathbf{W} = [\mathbf{Y}^* | \mathbf{X}^*]$, which implies that $\mathbf{W} \sim \mathcal{N}([\mu_{\mathbf{Y}^*} | \mu_{\mathbf{X}^*}], \mathbf{I}_n \otimes \Sigma)$, where

$$\Sigma = \begin{pmatrix} \Sigma_{11} & \Sigma_{12} \\ \Sigma_{21} & \Sigma_{22} \end{pmatrix}.$$

Finally, set $\mathbf{Z} = \mathbf{W} - [\mu_{\mathbf{Y}^*} | \mu_{\mathbf{X}^*}]$, thus $\mathbf{Z} = [\mathbf{Y} | \mathbf{X}] \sim \mathcal{N}(\mathbf{0}, \mathbf{I}_n \otimes \Sigma)$, where we have defined $\mathbf{Y} = \mathbf{Y}^* - \mu_{\mathbf{Y}^*}$ and $\mathbf{X} = \mathbf{X}^* - \mu_{\mathbf{X}^*}$.

Now, we are interested in the measure of the relation between the two variates \mathbf{X} and \mathbf{Y} , where $\Sigma_{12} = \Sigma'_{21}$ is the covariance matrix between the components of \mathbf{X} and the components of \mathbf{Y} . In order to establish that comparison we need to define the following supporting equivalent class of shapes.

Definition 2.1. Given two Helmertized $n \times s$ matrices \mathbf{X} and \mathbf{Y} , it is said that they have the same eulerian shape, if

1. $\mathbf{H}\mathbf{X} = [\mathbf{X}'_1 | \mathbf{0}]'$, where \mathbf{X}_1 is a non-singular $s \times s$ matrix and $\mathbf{H} \in O(r)$,
2. $\mathbf{H}\mathbf{Y} = \mathbf{T} = [\mathbf{U}' | \mathbf{V}']'$, where \mathbf{U} is $s \times s$, \mathbf{V} is $(r - s) \times s$ and \mathbf{H} is defined according to (1), and,
3. \mathbf{U} and \mathbf{V} satisfies $|(\mathbf{U}'\mathbf{U})(\mathbf{U}'\mathbf{U} + \mathbf{V}'\mathbf{V})^{-1} - \mathbf{I}_s| = 0$.

In this definition note that the matrix \mathbf{X} is of rank s , then there exists a rotation matrix $\mathbf{H} \in O(n)$ in order that $\mathbf{H}\mathbf{X} = [\mathbf{X}'_1 | \mathbf{0}]'$, where \mathbf{X}_1 is a non-singular $s \times s$ matrix, this matrix absorbs the eulerian meaningful shape of \mathbf{X} , and then the matrix \mathbf{Y} is rotated with that preceding orthogonal matrix, and partitioned according to $\mathbf{H}\mathbf{Y} = \mathbf{T} = [\mathbf{U}' | \mathbf{V}']'$, which must satisfy $|(\mathbf{U}'\mathbf{U})(\mathbf{U}'\mathbf{U} + \mathbf{V}'\mathbf{V})^{-1} - \mathbf{I}_s| = 0$. Observe also that \mathbf{U} and \mathbf{V} depend on \mathbf{X} .

The name of this class of shape obeys the type ${}_2F_1(\cdot)$ of the hypergeometric series involved in the main theorem of the present work.

We can put together the above transformations and definitions into the following steps which obtains the eulerian coordinates (\mathbf{U}, \mathbf{V}) of a given pair of original figures $(\mathbf{X}^{**}, \mathbf{Y}^{**})$:

$$\mathbf{L}(\mathbf{Y}^{**} \quad \mathbf{X}^{**}) = (\mathbf{Y}^* \quad \mathbf{X}^*) = \mathbf{W} = (\mathbf{Y} + \mu_{\mathbf{Y}^*} \quad \mathbf{X} + \mu_{\mathbf{X}^*}) \Rightarrow \begin{cases} \mathbf{H}\mathbf{X} = \begin{pmatrix} \mathbf{X}_1 \\ \mathbf{0} \end{pmatrix} \\ \mathbf{H}\mathbf{Y} = \begin{pmatrix} \mathbf{U} \\ \mathbf{V} \end{pmatrix} \end{cases},$$

subject to $|(\mathbf{U}'\mathbf{U})(\mathbf{U}'\mathbf{U} + \mathbf{V}'\mathbf{V})^{-1} - \mathbf{I}_s| = 0$.

Geometrically, Helmertized matrices means that \mathbf{Y}^* and \mathbf{X}^* are invariant under translation, and then with the remaining transformations, the resulting eulerian shape (\mathbf{U}, \mathbf{V}) of the pair $(\mathbf{X}^*, \mathbf{Y}^*)$ is all geometrical information remained after filtering out the rotation and permutations of the columns from the Helmertized pair $(\mathbf{X}^*, \mathbf{Y}^*)$.

This last property can be understood as the eulerian shape is invariant under the label of the axis of coordinates. For example, under this equivalent class, figures in an Euclidian three dimension space labeled with points with coordinates (x, y, z) are equivalent to figures with permuted the axis of coordinates, as (y, z, x) , (z, x, y) , (y, x, z) , (z, y, x) and (x, z, y) . This unusual invariance does not hold in the classical shapes via euclidian, affine or projective transformations and it is the most important novelty of the proposed approach, because does not require that the landmarks of the two objects strictly match in labels of the coordinates of axis.

The few works published in this area belong to procrustes methods based on unlabelled points where the minimizations of the distances between the figures are carried out over the

similarity transformations and permutations of the landmarks labels, they include a number of applications as megalithic standing stones (Cornwall) and human vision, among others, see section 12.9 of Dryden and Mardia (1998). As usual, the problems of inference and the exact density are one of the obstacles to solve in the existing approaches. Finally, this invariant statistics of shape analysis enters too into the so called landmark free approaches, a wider area of study, see for example section 12.10 of Dryden and Mardia (1998).

Clearly, with definition 2.1 we can implement classical procrustes analysis, as it was done for Euclidian and affine transformation, but we are interesting in the statistical analysis of the emergent shape.

In presence of randomness in the location of landmarks in the two Helmertized figures \mathbf{X} and \mathbf{Y} (linear transformations of the original figures \mathbf{X}^{**} and \mathbf{Y}^{**}), the so called squared canonical correlation coefficients allow the statistical matching of the objects via

$$|(\mathbf{Y}'\mathbf{Y})^{-1}\mathbf{Y}'\mathbf{X}(\mathbf{X}'\mathbf{X})^{-1}\mathbf{X}'\mathbf{Y} - r^2\mathbf{I}_K| = 0, \quad (1)$$

which is reduced to

$$|(\mathbf{U}'\mathbf{U})(\mathbf{U}'\mathbf{U} + \mathbf{V}'\mathbf{V})^{-1} - r^2\mathbf{I}_K| = 0, \quad (2)$$

by the items (1) and (2) of Definition 2.1.

As we proved, \mathbf{X} and \mathbf{Y} are the $n = N - 1 \times K$ helmertized matrices, such that $\mathbf{Y} \sim \mathcal{N}(\mathbf{0}, \mathbf{I}_n \otimes \mathbf{\Sigma}_{11})$, $\mathbf{X} \sim \mathcal{N}(\mathbf{0}, \mathbf{I}_n \otimes \mathbf{\Sigma}_{22})$ and we are interested in the measure of the relation between \mathbf{X} and \mathbf{Y} , where $\mathbf{\Sigma}_{12} = \mathbf{\Sigma}'_{21}$ is the covariance matrix between the components of \mathbf{X} and the components of \mathbf{Y} . Thus, $\mathbf{Z} = [\mathbf{Y}|\mathbf{X}] \sim \mathcal{N}(\mathbf{0}, \mathbf{I}_n \otimes \mathbf{\Sigma})$, where

$$\mathbf{\Sigma} = \begin{pmatrix} \mathbf{\Sigma}_{11} & \mathbf{\Sigma}_{12} \\ \mathbf{\Sigma}_{21} & \mathbf{\Sigma}_{22} \end{pmatrix}.$$

The invariant statistics involved in the shape theory context arrives here when we study the distribution of the so called squared canonical correlation coefficients under the Eulerian transformation above described, which obtains the squared canonical form of the covariance matrix as:

$$\mathbf{\Sigma} = \begin{pmatrix} \mathbf{I} & \mathbf{P} & \mathbf{0} \\ \mathbf{P} & \mathbf{I} & \mathbf{0} \\ \mathbf{0} & \mathbf{0} & \mathbf{I} \end{pmatrix}.$$

where \mathbf{P} is the $K \times K$ diagonal matrix with the squared canonical correlations ρ_1, \dots, ρ_K arranged in decreasing order down the diagonal (see Constantine (1963), Muirhead (1982), p. 539).

So, from theorem 11.3.2 of Muirhead (1982), p. 557 (see also Constantine (1963)), we have:

Let $\mathbf{A} = \mathbf{Z}'\mathbf{Z} = \begin{pmatrix} \mathbf{Y}'\mathbf{Y} & \mathbf{Y}'\mathbf{X} \\ \mathbf{X}'\mathbf{Y} & \mathbf{X}'\mathbf{X} \end{pmatrix} = \begin{pmatrix} \mathbf{A}_{11} & \mathbf{A}_{12} \\ \mathbf{A}_{21} & \mathbf{A}_{22} \end{pmatrix}$ have the $\mathcal{W}_{2K}(n, \mathbf{\Sigma})$ distribution, where $n \geq 2K$. Then the joint probability density function of r_1^2, \dots, r_K^2 , the latent roots of $\mathbf{A}_{11}^{-1}\mathbf{A}_{12}\mathbf{A}_{22}^{-1}\mathbf{A}_{21}$, is

$$\begin{aligned} f(r_1^2, \dots, r_K^2) &= \prod_{i=1}^K (1 - \rho_i^2)^{n/2} {}_2F_1^{(K)} \left(\frac{1}{2}n, \frac{1}{2}n; \frac{1}{2}K; \mathbf{P}^2, \mathbf{R}^2 \right) \\ &\times \frac{\pi^{K^2/2}}{\Gamma_K^2(\frac{1}{2}K)} \frac{\Gamma_K(\frac{1}{2}n)}{\Gamma_K[\frac{1}{2}(n-K)]} \\ &\times \prod_{i=1}^K \left[(r_i^2)^{-1/2} (1 - r_i^2)^{(n-2K-1)/2} \right] \prod_{i < j}^K (r_i^2 - r_j^2), \end{aligned}$$

for $1 > r_1^2 > \dots > r_K^2 > 0$, where $\rho_1^2, \dots, \rho_K^2$ are the latent roots of $\mathbf{\Sigma}_{11}^{-1}\mathbf{\Sigma}_{12}\mathbf{\Sigma}_{22}^{-1}\mathbf{\Sigma}_{21}$, $\mathbf{P}^2 = \text{diag}(\rho_1^2, \dots, \rho_K^2)$ and $\mathbf{R}^2 = \text{diag}(r_1^2, \dots, r_K^2)$.

3 The main result

For decades, the above type of expressions could not be computed and they forced us to asymptotic studies (see section 11.3.5 of Muirhead (1982)), and it seems that with the recent algorithms of Koev and Edelman (2006) the exact distribution can be used for applications. However, recently Caro-Lopera et al. (2014c), proved that those algorithms do not converge when the inference is performed in certain shape invariants as the affine case even applied to small size landmark data.

Computation in matrix variate theory via zonal polynomials (see Muirhead (1982)) and invariant polynomials of several matrix arguments extending the preceding ones (Davis (1979), Davis (1980)) has been the biggest problem in such area, there are hundreds of papers deriving numbers of theoretical properties involving such polynomials or asymptotic distributions, etc. but a very few, considering the problem of inference with the exact densities. For decades the zonal polynomials were impossible to compute until the works of Koev and Edelman (2006), meanwhile the computation of invariant polynomials of Davis remains unsolved since 1979. However, infinite series of zonal polynomials has considerable problems and so the performance of inference associated to the large number of results.

The problem for the computation of one hypergeometric series is addressed by Koev and Edelman (2006) in page 845 : “Several problems remain open, among them automatic detection of convergence”. This difficulty is amplified when we have to consider the optimization of a large product of such hypergeometric series, and the addressed algorithms do not allow large truncations to obtain certain accuracy and the convergence is completely doubtful.

So, in this scenario we have two ways to follow, a computational study which involves also a machine problem or trying an analytical solution.

Motivated by a similar situation in affine shape studied by Caro-Lopera et al. (2014c), this section attends an analytical solution to the problem of Eulerian shape inference. As before, the solution resides in the fact that shape densities are usually infinite series of zonal polynomials, but a few of them can be studied in the setting of the so called polynomial shape densities, which exploits some characteristics of the parameters of the distributions indexed by the number of landmarks and dimensions, and by using matrix generalized matrix relations, the density can be turned into a polynomial. For example, the affine shape theory is characterized by a confluent hypergeometric function type which can be turned into a polynomial density by some special domain and using the so called generalized matrix Kummer relation of Díaz-García and Caro-Lopera (2015), a generalization of the well known Kummer relation by Herz (1955) with gaussian kernel. Continuing in this way, we expect that the next type of hypergeometric shape distribution, the Eulerian of this paper could be transformed into a polynomial by using some special parametric space and the similar Euler matrix relations. However, the density derived in the previous section is a modified Eulerian hypergeometric type and involves two matrix arguments instead the expected one, which facilitates the automatic application of the Euler matrix relations. Given the connection between the Eulerian shape density and the squared canonical correlation result of Constantine (1963), it seems that non existence of that relations explains why the last result was set as an infinite series of products of zonal polynomials, instead as a polynomial of low degree, as it happens with a number of result based on Gaussian distributions and Kummer relations. Then an improvement of the shape density will be applied in the squared canonical correlation theory too.

Specifically, recall that the hypergeometric function of two $m \times m$ matrices \mathbf{X} and \mathbf{Y} as

arguments are given by

$${}_pF_q^{(m)}(a_1, \dots, a_p; b_1, \dots, b_q; \mathbf{X}, \mathbf{Y}) = \sum_{k=0}^{\infty} \sum_{\kappa} \frac{(a_1)_{\kappa} \cdots (a_p)_{\kappa}}{(b_1)_{\kappa} \cdots (b_q)_{\kappa}} \frac{C_{\kappa}(\mathbf{X})C_{\kappa}(\mathbf{Y})}{k!C_{\kappa}(\mathbf{I}_m)}. \quad (3)$$

The problem is reduced to obtain certain matrix relation which turns certain series of the type ${}_2F_1^{(m)}(a, b; c; \mathbf{X}, \mathbf{Y})$ into an expression of the type $f(c - a, b; c; \mathbf{X}, \mathbf{Y})$ in such way that $c - a$ are negative integers or negative half-integers, which will turn $f(\cdot)$ into a polynomial of low degree.

The required computable is obtained from the following matrix relation due to Caro-Lopera (2014):

$${}_2F_1^{(m)}(a_1, a_2; b_1; \mathbf{X}, \mathbf{Y}) = \sum_{k=0}^{\infty} \frac{1}{k!} \sum_{\kappa} \frac{(b_1 - a_1)_{\kappa} (a_2)_{\kappa}}{(b_1)_{\kappa}} \times \int_{O(m)} |\mathbf{I}_m - \mathbf{XHYH}'|^{-a_2} C_{\kappa}(-\mathbf{XHYH}'(\mathbf{I}_m - \mathbf{XHYH}')^{-1})(d\mathbf{H}); \quad (4)$$

if $b_1 - a_1$ is a negative integer, say $-q$, the hypergeometric function is a polynomial of degree mq .

And given that $n = N - 1 (\geq 2K)$ is the number of helmertized landmarks in K dimension, then $\frac{K}{2} - \frac{n}{2} = (K - N + 1)/2$ is a negative integer or a half negative integer, so we have arrive to main result of this work:

Theorem 3.1. *Let $\mathbf{A} = \mathbf{Z}'\mathbf{Z} = \begin{pmatrix} \mathbf{Y}'\mathbf{Y} & \mathbf{Y}'\mathbf{X} \\ \mathbf{X}'\mathbf{Y} & \mathbf{X}'\mathbf{X} \end{pmatrix} = \begin{pmatrix} \mathbf{A}_{11} & \mathbf{A}_{12} \\ \mathbf{A}_{21} & \mathbf{A}_{22} \end{pmatrix}$ have the $\mathcal{W}_{2K}(n, \Sigma)$ distribution, where $n \geq 2K$. Then the joint probability density function of r_1^2, \dots, r_K^2 , the latent roots of $\mathbf{A}_{11}^{-1}\mathbf{A}_{12}\mathbf{A}_{22}^{-1}\mathbf{A}_{21}$, is*

$$f(r_1^2, \dots, r_K^2) = \frac{\pi^{K^2/2}}{\Gamma_K^2(\frac{1}{2}K)} \frac{\Gamma_K(\frac{1}{2}n)}{\Gamma_K[\frac{1}{2}(n-K)]} \prod_{i=1}^K (1 - \rho_i^2)^{n/2} \prod_{i < j}^K (r_i^2 - r_j^2) \times \prod_{i=1}^K \left[(r_i^2)^{-1/2} (1 - r_i^2)^{(n-2K-1)/2} \right] \sum_{l=0}^{\infty} \frac{1}{l!} \sum_{\lambda} \frac{\left(\frac{K}{2} - \frac{n}{2}\right)_{\lambda} \left(\frac{n}{2}\right)_{\lambda}}{\left(\frac{K}{2}\right)_{\lambda}} \times \int_{O(K)} |\mathbf{I}_K - \mathbf{P}^2\mathbf{H}\mathbf{R}^2\mathbf{H}'|^{-n/2} C_{\lambda}(-\mathbf{P}^2\mathbf{H}\mathbf{R}^2\mathbf{H}'(\mathbf{I}_K - \mathbf{P}^2\mathbf{H}\mathbf{R}^2\mathbf{H}')^{-1})(d\mathbf{H}),$$

for $1 > r_1^2 > \dots > r_1^K > 0$, where $\rho_1^2, \dots, \rho_K^2$ are the latent roots of $\Sigma_{11}^{-1}\Sigma_{12}\Sigma_{22}^{-1}\Sigma_{21}$, $\mathbf{P}^2 = \text{diag}(\rho_1^2, \dots, \rho_K^2)$ and $\mathbf{R}^2 = \text{diag}(r_1^2, \dots, r_K^2)$. If $\frac{K}{2} - \frac{n}{2}$ is a negative integer, say $-q$, the function is a polynomial of degree Kq in K variables.

Note that the parametric condition of Eulerian polynomial shape, i.e. $\frac{K}{2} - \frac{n}{2}$, ($n \geq 2K$) just demands that the objects in K -even(odd) dimensions are summarized by a number of N -odd(even) anatomical landmarks.

Nevertheless the most of the literature of statistical shape analysis is valid for any dimension K , the application of the theory seems to be very restricted to anatomical landmarks placed on two and three dimensional objects, in fact the classical text on shape theory, such as Dryden and Mardia (1998) only uses 2-D landmark data, and 3-D applications are very rarely given the complexity of the distributions and the registration of invariant critical points. So, when we consider $K = 2$, all the typical landmark data presented for example in Dryden and Mardia (1998) can be studied and the integral over the orthogonal group

is a feasible and programming task using the exact formulae for Jack polynomials (which includes real zonal polynomials) due to Caro-Lopera *et al* (2007).

Next we give some summary of Jack polynomials and exact two dimensional formulae, which particularized to zonal polynomials, will be needed in some applications.

Let us characterize the Jack symmetric function $J_\kappa^{(\alpha)}(y_1, \dots, y_m)$ of parameter α , see Sawyer (1997). Consider a decreasing sequence of nonnegative integers $\kappa = (k_1, k_2, \dots)$ with only finitely many nonzero terms is said to be a partition of $k = \sum k_i$. Let κ and $\lambda = (l_1, l_2, \dots)$ be two partitions of k . We write $\lambda \leq \kappa$ if $\sum_{i=1}^t l_i \leq \sum_{i=1}^t k_i$ for each t . The conjugate of κ is $\kappa' = (k'_1, k'_2, \dots)$ where $k'_i = \text{card}\{j : k_j \geq i\}$. The length of κ is $l(\kappa) = \max\{i : k_i \neq 0\} = k'_1$. If $l(\kappa) \leq m$, one often writes $\kappa = (k_1, k_2, \dots, k_m)$. The partition $(1, \dots, 1)$ of length m will be denoted by 1_m .

And recall that the monomial symmetric function $M_\kappa(\cdot)$ indexed by a partition κ can be regarded as a function of an arbitrary number of variables such that all but a finite number are equal to 0: if $y_i = 0$ for $i > m \geq l(\kappa)$ then $M_\kappa(y_1, \dots, y_m) = \sum y_1^{\sigma_1} \cdots y_m^{\sigma_m}$, where the sum is over all distinct permutations $\{\sigma_1, \dots, \sigma_m\}$ of $\{k_1, \dots, k_m\}$, and if $l(\kappa) > m$ then $M_\kappa(y_1, \dots, y_m) = 0$. A symmetric function f is a linear combination of monomial symmetric functions. If f is a symmetric function then $f(y_1, \dots, y_m, 0) = f(y_1, \dots, y_m)$. For each $m \geq 1$, $f(y_1, \dots, y_m)$ is a symmetric polynomial in m variables.

Thus the Jack symmetric function $J_\kappa^{(\alpha)}(y_1, \dots, y_m)$ with a parameter α , satisfy the following conditions:

$$J_\kappa^{(\alpha)}(y_1, \dots, y_m) = \sum_{\lambda \leq \kappa} j_{\kappa, \lambda} M_\lambda(y_1, \dots, y_m), \quad (5)$$

$$J_\kappa^{(\alpha)}(1, \dots, 1) = \alpha^k \prod_{i=1}^m \binom{m-i+1}{\alpha}_{k_i}, \quad (6)$$

$$\begin{aligned} \sum_{i=1}^m y_i^2 \frac{\partial^2 J_\kappa^{(\alpha)}(y_1, \dots, y_m)}{\partial y_i^2} + \frac{2}{\alpha} \sum_{i=1}^m y_i^2 \sum_{j \neq i} \frac{1}{y_i - y_j} \frac{\partial J_\kappa^{(\alpha)}(y_1, \dots, y_m)}{\partial y_i} = \\ \sum_{i=1}^m k_i (k_i - 1 + \frac{2}{\alpha} (m - i)) J_\kappa^{(\alpha)}(y_1, \dots, y_m). \end{aligned} \quad (7)$$

Here the constants $j_{\kappa, \lambda}$ do not dependent on y_i 's but on κ and λ , and $(a)_n = \prod_{i=1}^n (a + i - 1)$. Note that if $m < l(\kappa)$ then $J_\kappa^{(\alpha)}(y_1, \dots, y_m) = 0$. The conditions include the case $\alpha = 0$ and then $J_\kappa^{(0)}(y_1, \dots, y_m) = e_{\kappa'} \prod_{i=1}^m (m - i + 1)^{k_i}$, where $e_\kappa(y_1, \dots, y_m) = \prod_{i=1}^{l(\kappa)} e_{k_i}(y_1, \dots, y_m)$ are the elementary symmetric functions indexed by partitions κ , if $m \geq l(\kappa)$ then $e_r(y_1, \dots, y_m) = \sum_{i_1 < i_2 < \dots < i_r} y_{i_1} \cdots y_{i_r}$, and if $m < l(\kappa)$ then $e_r(y_1, \dots, y_m) = 0$, see Sawyer (1997).

Now, from Koev and Edelman (2006), the Jack functions $J_\kappa^{(\alpha)}(\mathbf{Y}) = J_\kappa^{(\alpha)}(y_1, \dots, y_m)$, with y_1, \dots, y_m being the eigenvalues of the matrix \mathbf{Y} , can be normalized in such a way that

$$\sum_{\kappa} C_\kappa^\alpha(\mathbf{Y}) = (\text{tr}(\mathbf{Y}))^k,$$

where $C_\kappa^\alpha(\mathbf{Y})$ denotes the Jack polynomials. They are related to the Jack functions by

$$C_\kappa^\alpha(\mathbf{Y}) = \frac{\alpha^k k!}{j_\kappa} J_\kappa^\alpha(\mathbf{Y}), \quad (8)$$

where

$$j_\kappa = \prod_{(i, j) \in \kappa} h_*^\kappa(i, j) h_\kappa^*(i, j),$$

and $h_*^\kappa(i, j) = k_j - i + \alpha(k_i - j + 1)$ and $h_\kappa^*(i, j) = k_j - i + 1 + \alpha(k_i - j)$ are the upper and lower hook lengths at $(i, j) \in \kappa$, respectively.

Then by applying (8), we can write (7) as

$$\sum_1^m y_i^2 \frac{\partial^2 C_\kappa^{(\alpha)}(\mathbf{Y})}{\partial y_i^2} + \frac{2}{\alpha} \sum_{i=1}^m y_i^2 \sum_{j \neq i} \frac{1}{y_i - y_j} \frac{\partial C_\kappa^{(\alpha)}(\mathbf{Y})}{\partial y_i} = \sum_{i=1}^m k_i(k_i - 1 + \frac{2}{\alpha}(m - i)) C_\kappa^{(\alpha)}(\mathbf{Y}). \quad (9)$$

Now, when $m = 2$ in (9), Caro-Lopera *et al* (2007) found the following formulae for Jack Polynomials of the Second Order

$$\begin{aligned} \frac{C_{(k_1, k_2)}^{(\alpha)}(\mathbf{Y})}{C_{(k_1, k_2)}^{(\alpha)}(\mathbf{I}_2)} &= (y_1 y_2)^{(k_1 + k_2)/2} A_1 F\left(-\frac{\rho}{2}, \frac{\rho}{2} + \frac{1}{\alpha}; \frac{1}{2}; \frac{(y_1 + y_2)^2}{4y_1 y_2}\right) \\ &+ \frac{(y_1 y_2)^{(k_1 + k_2 - 1)/2}}{2(y_1 + y_2)^{-1}} A_2 F\left(\frac{1}{\alpha} + \frac{1 + \rho}{2}, \frac{1}{2} - \frac{\rho}{2}; \frac{3}{2}; \frac{(y_1 + y_2)^2}{4y_1 y_2}\right), \end{aligned} \quad (10)$$

with ρ being either even or odd. For distinguishing the case under consideration, odd or even, we will use the upper indices o or e with A_1 and A_2 . Then the corresponding solutions are the following

Even case. If $\rho = k_1 - k_2 = 2n$, $n = 0, 1, 2, \dots$ then

$$A_1^e = \frac{(-1)^n \prod_{i=0}^{n-1} (1 + 2i)}{\prod_{i=0}^{n-1} \left(1 + 2\left(\frac{1}{\alpha} + i\right)\right)} \quad \text{and} \quad A_2^e = 0.$$

Odd case. If $\rho = k_1 - k_2 = 2n + 1$, $n = 0, 1, 2, \dots$ then

$$A_1^o = 0 \quad \text{and} \quad A_2^o = (2n + 1)A_1^e.$$

Three particular cases are of interest in the literature: the quaternionic case ($\alpha = 1/2$), the complex zonal polynomials ($\alpha = 1$) and the real zonal polynomials ($\alpha = 2$), these results are summarized in the following table:

α	ρ	a	b	c	A_1	A_2
$\frac{1}{2}$	even	$-n$	$n+2$	$\frac{1}{2}$	$\frac{(-1)^n 3}{(2n+1)(2n+3)}$	0
	odd	$n+3$	$-n$	$\frac{3}{2}$	0	$\frac{(-1)^n 3}{(2n+3)}$
1	even	$-n$	$n+1$	$\frac{1}{2}$	$\frac{(-1)^n}{(2n+1)}$	0
	odd	$n+2$	$-n$	$\frac{3}{2}$	0	$(-1)^n$
2	even	$-n$	$n+1/2$	$\frac{1}{2}$	$\frac{(-1)^n (2n)!}{2^{2n} (n!)^2}$	0
	odd	$n+3/2$	$-n$	$\frac{3}{2}$	0	$\frac{(-1)^n (2n+1)!}{2^{2n} (n!)^2}$

The above formula for the real zonal polynomials corresponds to that derived by James (1968) and for the complex zonal polynomials, obtained by Caro-Lopera *et al* (2006), meanwhile it is the first appearance of an exact formulae for quaternionic polynomials.

So, finally, for the integration demanded in Theorem 3.1 over the orthogonal group $O(2)$ with respect the normalized invariant measure ($d\mathbf{H}$), we just follow the usual parametrization techniques, see for example Muirhead (1982).

4 Applications

In this section we describe the general procedure for applications of the Eulerian shape distributions and compare the computational performance when the inference of a certain appropriate landmark data for this data is studied under the modified classical result of Constantine (1963) via the algorithms of Koev and Edelman (2006) and the exact polynomial distribution here derived.

For the first aspect, there are a number of situations to consider, for example, the Eulerian shape can be used to establish correlation structure of two populations, or determine the correlation structure of a population and a given template, also, the correlation structure of a population and a given object probably belonging to another population, and finally, we can use the polynomial distributions for exploring the problem of landmark discrimination. Next we explain the associated procedure of each one.

4.1 Correlation structure of two populations

Consider a sample of m figures of a population \mathbf{X} and m figures of a population \mathbf{Y} ; both samples satisfying the shape invariance assumed for the Eulerian shape and the fact that $(K - N + 1)/2$, $(N - 1 \geq 2K)$ is a negative integer, i.e. the objects in K -even(odd) dimensions are summarized by a number of N -odd(even) anatomical landmarks. For each pair of figures $\mathbf{Z} = [\mathbf{Y}|\mathbf{X}]$ compute the corresponding $r_{1,j}^2, \dots, r_{K,j}^2$, $j = 1, \dots, m$ the latent roots of $\mathbf{A}_{11}^{-1} \mathbf{A}_{12} \mathbf{A}_{22}^{-1} \mathbf{A}_{21}$, in order to obtain the function $f_j(r_1^2, \dots, r_K^2)$ of Theorem 3.1.

Then maximize the likelihood function

$$L(\rho_1^2, \dots, \rho_K^2) = \prod_{j=1}^m f_j(r_1^2, \dots, r_K^2)$$

respect to the population squared canonical correlation coefficients $\rho_1^2, \dots, \rho_K^2$.

These estimates will provide the strength of relationship between the two populations in the sense of the Eulerian shape invariance.

As we shall see in the experiments various methods can be implemented in order to obtain more information about the shape equality of both populations without using the classical statistics for means, instead we can use the exact distribution of certain template vs one of the population and obtain the probability than an extreme correlation structure of the other population influenced by the same template, can be occurred.

4.2 Correlation structure of a population and a given template

Exactly as before, but in this case, we have m repeated templates \mathbf{X} and we want to verify the correlation between the population \mathbf{Y} and the template \mathbf{X} under the Eulerian shape assumptions.

4.3 Correlation structure of a population and a given figure

Exactly as before, but in this case, we have m repeated figures \mathbf{X} and we want to verify the correlation between the population \mathbf{Y} and a given “figure” \mathbf{X} , i.e. it can explain, under the requirements of the Eulerian invariants, if the last one belongs or not to the population \mathbf{Y} .

4.4 Landmark discrimination

This is one of the main less studied problems in the shape theory. It concerns the reduction of set of landmarks for a given figure without changing the explanation of the object. In other words it worries about reduction of dimensionality of a figure and set the shape theory in the domain of very low dimensions. The method of the preceding section can be used in order to study the landmark discrimination. To get this end, we start with figures \mathbf{Y} and \mathbf{X} (in any of the three possible scenarios explained in the above items) with a large number of landmarks N (not necessary anatomical landmarks, they can be mathematical or pseudolandmarks), estimate the corresponding ρ 's, then reduce the number of landmarks and repeat the estimation until the ρ 's change drastically, then we reach an optimal number of landmarks which summaries properly the object.

This technique is particular appropriate for shape analysis involving mathematical or pseudomathematical landmarks, which usually are equally-placed in the contour of the object. For example, the method is applicable in some extreme cases, such as discrimination of classes of potatoes or differentiation of non regular objects with no chance of placing anatomical landmarks objects. A profuse study of this landmark discrimination methodology is will be carried out in a subsequent work. Another useful application under consideration tries an automatic detection of anatomical landmarks using their limit from pseudo critical points. For example, the 46 pseudo-landmarks defined by Dryden and Mardia (1998) in the contour of the mouse vertebrae can be used for studying the discrimination problem and finding the possible optimal set of six anatomical landmarks usually referred in literature.

4.5 An application in postcode recognition

We end this section by illustrating the addressed problem of inference with the distribution provided by Constantine (1963) and the algorithms for hypergeometric functions by Koev and Edelman (2006). Then we compare the above results with the polynomial density here derived.

We select a known landmark data of literature on postcode recognition which has presented problems in inference using another shape invariants as the affine shape, see Caro-Lopera et al. (2014c).

In this case, we have a 30 sample of handwritten digit 3 (see Figure 1), with $N = 13$, ($K = 2$) landmarks placed according an equally spaced two joint octagons as a template (see Figure 2). We are interested in estimating the strength the estimate of correlation structure between the template and the handwritten digit 3. The main theorem can be used to obtain the estimates of population squared canonical correlations ρ_1^2 and ρ_2^2 by optimizing the corresponding likelihood. In this case the distribution is a polynomial of degree $-\frac{1}{2}(K - N + 1) \times K = 10$ in the two latent roots of the matrix argument in the zonal polynomial.

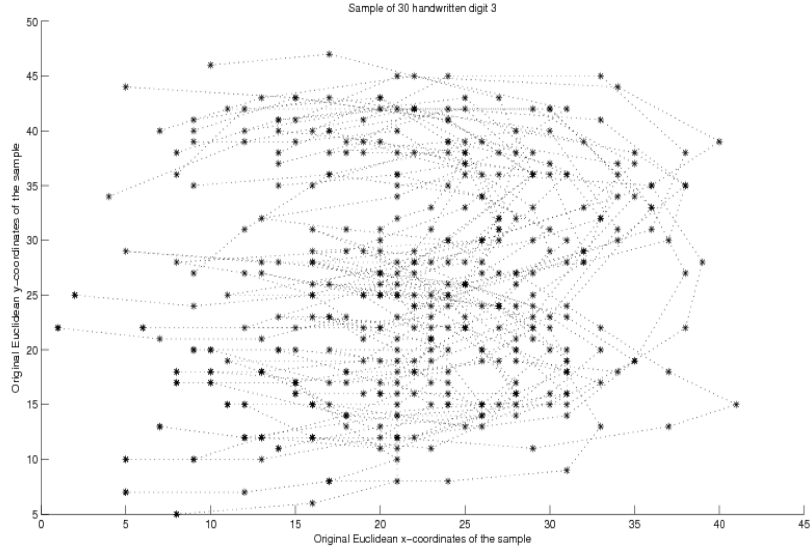


Figure 1: 30 handwritten digit 3.

If we truncate the original distributions derived by Constantine (1963) and use the algorithms of Koev and Edelman (2006) we obtain the following table, which shows the starting point (r_{1i}^2, r_{2i}^2) for the optimization, the population estimate coefficients between the template and the handwritten digit 3, the convergence and the number of iterations of the algorithm. In this case we just truncate the infinite series of zonal polynomials at 10th degree in order to compare the performance with the polynomial of 10-th degree which provides the solution. The computations were performed with a processor Intel(R) Core(TM)2 Duo CPU, E7400@2.80GHz, and 2,96GB of RAM.

r_{1i}^2	r_{2i}^2	Fval.	Conv.	Iter.	$\hat{\rho}_1^2$	$\hat{\rho}_2^2$
0.1	0.1	372.8472	y	23	0.1260	0.1260
0.1	0.2	372.8472	y	23	0.1260	0.1260
0.1	0.3	372.8472	y	27	0.1260	0.1260
0.1	0.4	372.8472	y	30	0.1260	0.1259
0.1	0.5	372.8472	y	44	0.1260	0.1260
0.1	0.6	372.8472	y	31	0.1260	0.1260
0.1	0.7	372.8472	y	31	0.1260	0.1260
0.1	0.8	372.8472	y	32	0.1260	0.1260
0.1	0.9	-	n	-	-	-

r_{1i}^2	r_{2i}^2	Fval.	Conv.	Iter.	$\hat{\rho}_1^2$	$\hat{\rho}_2^2$
0.2	0.2	372.8472	y	27	0.1260	0.1260
0.2	0.3	372.8472	y	34	0.1259	0.1260
0.2	0.4	372.8472	y	32	0.1259	0.1259
0.2	0.5	372.8472	y	37	0.1259	0.1260
0.2	0.6	372.8472	y	36	0.1260	0.1260
0.2	0.7	-	n	-	-	-
0.2	0.8	-	n	-	-	-
0.2	0.9	-	n	-	-	-

r_{1i}^2	r_{2i}^2	Fval.	Conv.	Iter.	$\hat{\rho}_1^2$	$\hat{\rho}_2^2$
0.3	0.3	372.8472	y	29	0.1260	0.1260
0.3	0.4	372.8472	y	39	0.1260	0.1260
0.3	0.5	372.8472	y	40	0.1260	0.1260
0.3	0.6	-	n	-	-	-
0.3	0.7	-	n	-	-	-
0.3	0.8	-	n	-	-	-
0.3	0.9	-	n	-	-	-

r_{1i}^2	r_{2i}^2	Fval.	Conv.	Iter.	$\hat{\rho}_1^2$	$\hat{\rho}_2^2$
0.4	0.4	-	n	-	-	-
0.4	0.5	372.8472	y	40	0.1260	0.1260
0.4	0.6	-	n	-	-	-
0.4	0.7	-	n	-	-	-
0.4	0.8	-	n	-	-	-
0.4	0.9	-	n	-	-	-

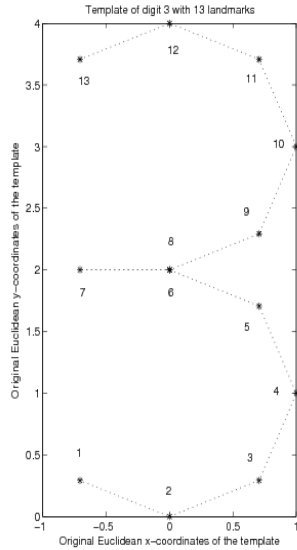


Figure 2: Configuration template.

r_{1i}^2	r_{2i}^2	Fval.	Conv.	Iter.	$\hat{\rho}_1^2$	$\hat{\rho}_2^2$
0.5	0.5	-	n	-	-	-
0.5	0.6	372.8472	y	37	0.1260	0.1260
0.5	0.7	-	n	-	-	-
0.5	0.8	-	n	-	-	-
0.5	0.9	-	n	-	-	-

r_{1i}^2	r_{2i}^2	Fval.	Conv.	Iter.	$\hat{\rho}_1^2$	$\hat{\rho}_2^2$
0.6	0.6	372.8472	y	34	0.1259	0.1260
0.6	0.7	372.8472	y	37	0.1260	0.1260
0.6	0.8	-	n	-	-	-
0.6	0.9	-	n	-	-	-

r_{1i}^2	r_{2i}^2	Fval.	Conv.	Iter.	$\hat{\rho}_1^2$	$\hat{\rho}_2^2$
0.7	0.7	-	n	-	-	-
0.7	0.8	-	n	-	-	-
0.7	0.9	-	n	-	-	-
0.8	0.8	-	n	-	-	-
0.8	0.9	-	n	-	-	-
0.9	0.9	-	n	-	-	-

There is no doubt that the algorithm does not work and cannot reach any credible solution; in fact for some starting points the algorithm does not converge even at a very low truncation of 10th degree.

Meanwhile the polynomial density gives a fast convergence no matters the starting point we consider, the result in this case by different classical methods for optimization, is: $\hat{\rho}_1^2 = 0.9542$ and $\hat{\rho}_2^2 = 0.6740$.

Now, if we want to approximate the exact result by using the result of Muirhead, the series must be truncated in a large number as the following table shows. We highlight that the algorithm was intervened many times in the starting point in order to obtain an stable solution.

Truncation	$\hat{\rho}_1^2$	$\hat{\rho}_2^2$	Truncation	$\hat{\rho}_1^2$	$\hat{\rho}_2^2$	Truncation	$\hat{\rho}_1^2$	$\hat{\rho}_2^2$
20	0.5890	0.5889	120	0.9246	0.6697	220	0.9484	0.6733
40	0.7319	0.7318	140	0.9330	0.6710	240	0.9500	0.6735
60	0.8554	0.6713	160	0.9389	0.6719	260	0.9512	0.6736
80	0.8922	0.6670	180	0.9431	0.6725	280	0.9521	0.6736
100	0.9121	0.6682	200	0.9461	0.6730	300	0.9527	0.6737

Truncation	$\hat{\rho}_1^2$	$\hat{\rho}_2^2$	Truncation	$\hat{\rho}_1^2$	$\hat{\rho}_2^2$
320	0.9531	0.6737	420	0.9538	0.6737
340	0.9534	0.6737	440	0.9538	0.6737
360	0.9536	0.6737	460	0.9539	0.6736
380	0.9537	0.6737	480	0.9539	0.6737
400	0.9538	0.6736	500	0.9539	0.6737

With the implemented routines based on infinite series of zonal polynomials was impossible to

reach the solution obtained with the exact distribution. After extremely large truncation of 500 they could not stabilize to the solution obtained with exact polynomial of 10-th degree. Note, that we cannot provide an analytical of numerical relationship between the truncation and the estimates, it is exactly the open problem addressed by Koev and Edelman (2006).

Once the computation problem is solved, we must pay attention to the interpretation of the squared canonical correlation estimates, $\hat{\rho}_1^2 = 0.9542$ and $\hat{\rho}_2^2 = 0.6740$, corresponding to the comparison between the template and a typical handwritten sample of digit 3. The first approach consist of computing the probability that a given handwritten digit 3 with particular r_{t1}^2 and r_{t2}^2 is far from the template, in this case we just need to compute $P((r_1^2, r_2^2) > (r_{t1}^2, r_{t2}^2))$, which is a feasible task by using the polynomial densities of Theorem 3.1.

Now, to obtain a measure for interpretation, we can apply the same procedure to a non-template object, for example, any handwritten digit 3 selected at random, see Figure 3; the next table summarizes the convergent problem of optimization when we use the infinite series. First we demonstrate the inefficient of the series which is truncated at the level of the degree 10-th of the exact polynomial distribution.

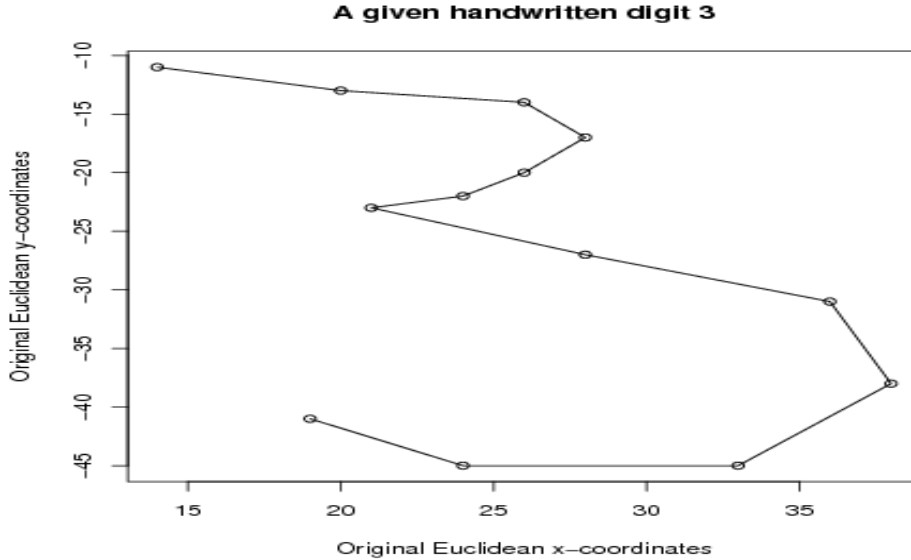


Figure 3: A randomly selected handwritten digit 3.

r_{1i}^2	r_{2i}^2	Fval.	Conv.	Iter.	$\hat{\rho}_1^2$	$\hat{\rho}_2^2$
0.1	0.1	553.8395	y	24	0.1283	0.1282
0.1	0.2	553.8395	y	24	0.1283	0.1282
0.1	0.3	553.8395	y	30	0.1282	0.1282
0.1	0.4	553.8395	y	33	0.1282	0.1283
0.1	0.5	553.8395	y	35	0.1282	0.1282
0.1	0.6	553.8395	y	32	0.1282	0.1282
0.1	0.7	553.8395	y	31	0.1282	0.1282
0.1	0.8	553.8395	y	34	0.1283	0.1282
0.1	0.9	-	n	-	-	-

r_{1i}^2	r_{2i}^2	Fval.	Conv.	Iter.	$\hat{\rho}_1^2$	$\hat{\rho}_2^2$
0.2	0.2	553.8395	y	26	0.1282	0.1282
0.2	0.3	553.8395	y	34	0.1282	0.1282
0.2	0.4	553.8395	y	33	0.1282	0.1282
0.2	0.5	553.8395	y	38	0.1282	0.1282
0.2	0.6	553.8395	y	38	0.1282	0.1283
0.2	0.7	-	n	-	-	-
0.2	0.8	-	n	-	-	-
0.2	0.9	-	n	-	-	-

r_{1i}^2	r_{2i}^2	Fval.	Conv.	Iter.	$\hat{\rho}_1^2$	$\hat{\rho}_2^2$
0.3	0.3	553.8395	y	30	0.1282	0.1282
0.3	0.4	553.8395	y	37	0.1282	0.1283
0.3	0.5	553.8395	y	37	0.1282	0.1283
0.3	0.6	553.8395	y	36	0.1283	0.1282
0.3	0.7	-	n	-	-	-
0.3	0.8	-	n	-	-	-
0.3	0.9	-	n	-	-	-

r_{1i}^2	r_{2i}^2	Fval.	Conv.	Iter.	$\hat{\rho}_1^2$	$\hat{\rho}_2^2$
0.4	0.4	-	n	-	-	-
0.4	0.5	553.8395	y	39	0.1282	0.1282
0.4	0.6	-	n	-	-	-
0.4	0.7	-	n	-	-	-
0.4	0.8	-	n	-	-	-
0.4	0.9	-	n	-	-	-

r_{1i}^2	r_{2i}^2	Fval.	Conv.	Iter.	$\hat{\rho}_1^2$	$\hat{\rho}_2^2$
0.5	0.5	-	n	-	-	-
0.5	0.6	553.8395	y	36	0.1282	0.1282
0.5	0.7	-	n	-	-	-
0.5	0.8	-	n	-	-	-
0.5	0.9	-	n	-	-	-

r_{1i}^2	r_{2i}^2	Fval.	Conv.	Iter.	$\hat{\rho}_1^2$	$\hat{\rho}_2^2$
0.6	0.6	-	n	-	-	-
0.6	0.7	553.8395	y	40	0.1282	0.1282
0.6	0.8	-	n	-	-	-
0.6	0.9	-	n	-	-	-

r_{1i}^2	r_{2i}^2	Fval.	Conv.	Iter.	$\hat{\rho}_1^2$	$\hat{\rho}_2^2$
0.7	0.7	-	n	-	-	-
0.7	0.8	-	n	-	-	-
0.7	0.9	-	n	-	-	-
0.8	0.8	-	n	-	-	-
0.8	0.9	-	n	-	-	-
0.9	0.9	-	n	-	-	-

Again the malfunction of the algorithms is revealed in the simple truncation 10; no convergence is obtained for every starting point, in particular for the largest ones which are near to the mean. Each pair of solutions is so far from the estimates based on the exact density; those values were derived by different numerical methods, no problems of convergence was occurred and were independent of the starting points, the corresponding estimates are: $\hat{\rho}_1^2 = 0.9753$ and $\hat{\rho}_2^2 = 0.8748$.

If we want to pursuit that solution we require enormous values for truncating the series, as it is shown in the following table.

Truncation	$\hat{\rho}_1^2$	$\hat{\rho}_2^2$	Truncation	$\hat{\rho}_1^2$	$\hat{\rho}_2^2$	Truncation	$\hat{\rho}_1^2$	$\hat{\rho}_2^2$
20	0.5976	0.5976	120	0.8883	0.8882	220	0.9510	0.8709
40	0.7446	0.7446	140	0.9188	0.8728	240	0.9548	0.8711
60	0.8107	0.8107	160	0.9315	0.8708	260	0.9578	0.8714
80	0.8481	0.8480	180	0.9400	0.8704	280	0.9603	0.8717
100	0.8719	0.8718	200	0.9462	0.8706	300	0.9625	0.8719

Truncation	$\hat{\rho}_1^2$	$\hat{\rho}_2^2$	Truncation	$\hat{\rho}_1^2$	$\hat{\rho}_2^2$
320	0.9642	0.8721	480	0.9721	0.8729
340	0.9658	0.8724	500	0.9726	0.8729
360	0.9671	0.8725	520	0.9731	0.8729
380	0.9682	0.8726	540	0.9735	0.8729
400	0.9692	0.8727	560	0.9738	0.8729
420	0.9701	0.8727	580	0.9741	0.8729
440	0.9709	0.8728	600	0.9743	0.8729
460	0.9715	0.8728			

After a truncation of zonal polynomials of order greater than 600 the algorithm fails and no computational chance of reaching the estimation based on the exact polynomial distribution, is possible.

Summarizing we have arrive at two estimates: Template vs Handwritten digit 3, $\hat{\rho}_1^2 = 0.9542$ and $\hat{\rho}_2^2 = 0.6740$; meanwhile Given Handwritten digit 3 vs Handwritten digit 3, $\hat{\rho}_1^2 = 0.9753$ and $\hat{\rho}_2^2 = 0.8748$, the difference is notable, but a way for comparison can be the addressed distribution of Theorem 3.1. In this case we just compute the probability that an extreme correlation structure as $r_1^2 = 0.9753$ and $r_2^2 = 0.8748$ due to a particular given handwritten 3, occurs under the distribution of the correlation structure influenced by the template. In this case, integration of distribution of Theorem 3.1 provides that $P((r_1^2, r_2^2) > (0.9753, 0.8748)) < 0.0015$, which means that the Eulerian shape of the given handwritten digit 3 is so far from the usual template of number 3. Figure 4 shows the associated distribution of the template and an approximate region for integration.

4.6 An application in machine vision

We end this section by studying the Eulerian shape differentiation between two populations, the application can be useful in machinery vision. Consider two samples of 17 crackers as shown in figures 5 (cracker type A) and 6(cracker type B).

In cracker type A, we register 9 landmarks by hand, the five evident marks on the cracker and the four corners, see Figure 7. We try to place similar landmarks on cracker type B, corresponding to the four corners, the center and the four nearest holes to the corners, , see Figure 8. It is clear the notorious variance of placing this landmarks on cracker B versus the more easily registration on cracker A. For a complete process in machine vision, we can also use automatic corner detection as Harris' method for the landmark registration, but we want to increase intentional the difficulty of the pursuit population discrimination. Note also the adequacy of objects for implementing the Eulerian differentiation, the figures have strong symmetry and some flexibility of choosing the

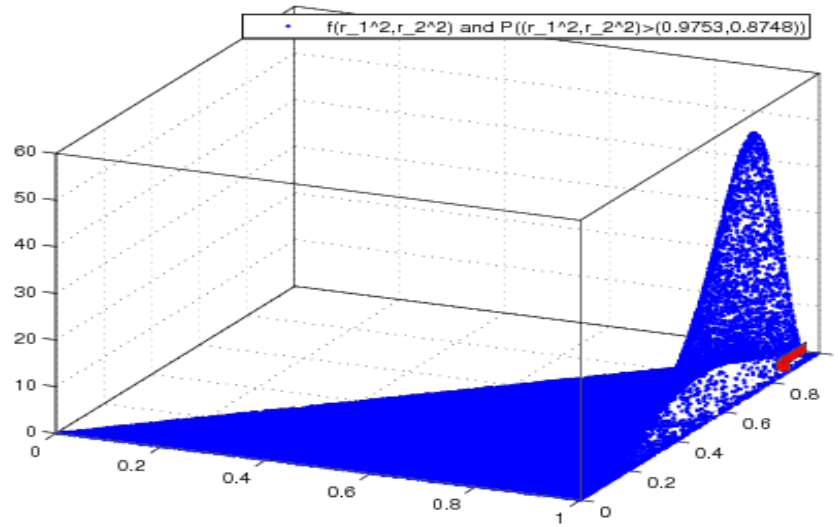


Figure 4: Eulerian polynomial joint distribution of template vs handwritten digit 3 and a test for a randomly selected handwritten code.



Figure 5: A 17-sample of crackers type A randomly selected, original objects.

landmark labels is allowed because the geometric invariants of such shape; meanwhile, in affine or similarity studies, the labeling have more radical constraint.

We ask for a significant difference in Eulerian shape between crackers A and B. Next we list the results of some approaches.



Figure 6: A 17-sample of crackers type B randomly selected, original objects.

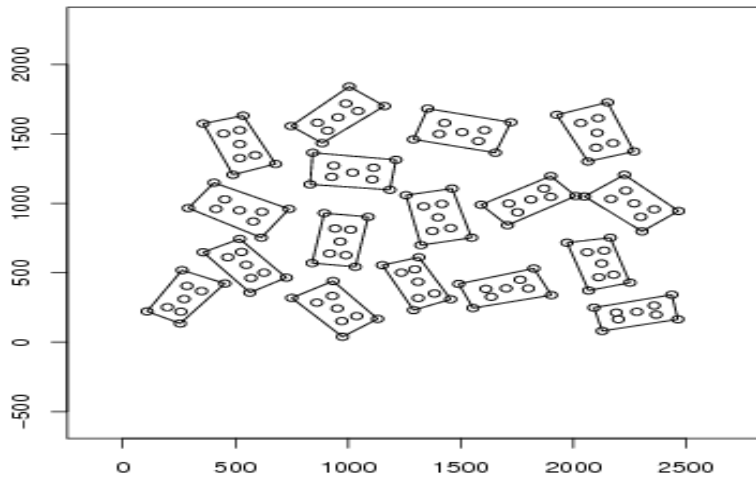


Figure 7: A 17-sample of crackers type A randomly selected with 9 landmarks.

METHOD 1: USING A DEGENERATED TEMPLATE:

We proceed with a similar methodology of the handwritten digit 3 landmark data. In this case the selected template is just a rectangle with its center, in such way that 5 of the 9 landmarks are concentrated in the geometrical center and the remaining ones are the vertices, see Figure 9. Corresponding estimates for population of cracker A are $\hat{\rho}_1^2 = 0.7959$ and $\hat{\rho}_2^2 = 0.7955$; meanwhile

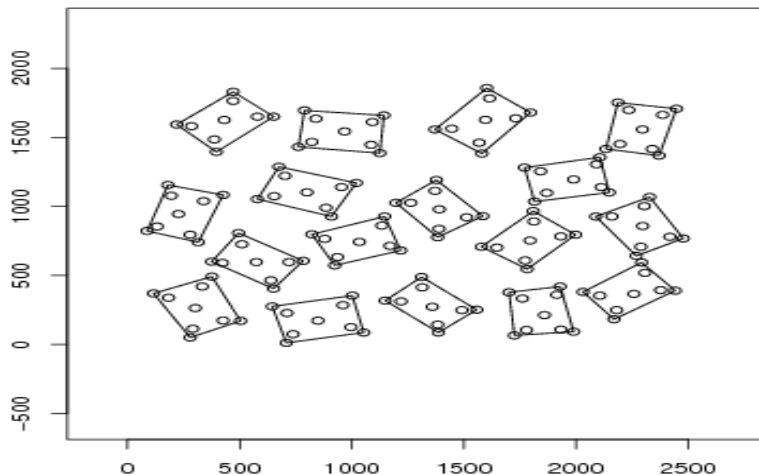


Figure 8: A 17-sample of crackers type B randomly selected with 9 landmarks.

estimates for population of cracker B are, $\hat{\rho}_1^2 = 0.6218$ and $\hat{\rho}_2^2 = 0.6212$, as we expect, the template is a little more correlated with cracker A than cracker B. In this case we just compute the probability that an extreme correlation structure as $r_1^2 = 0.7959$ and $r_2^2 = 0.7955$ due to population correlation structure estimates of cracker B with the given template, occurs under the distribution of the correlation structure influenced by the template and population of cracker A. After integration of distribution of Theorem 3.1 we have that $P((r_1^2, r_2^2) > (0.7959, 0.7955)) < 0.0141$, which means that the Eulerian shape of cracker B is different from the Eulerian shape of cracker A, even under such degenerated template with more than 50 percent of coincident landmarks. Figure 10 shows the associated distribution of the template and an approximate region for integration.

METHOD 2: USING A SIMILAR TEMPLATE TO CRACKER A:

If we select a template where 4 of the above coincident landmarks are equally spaced in the diagonals of the rectangle (very similar to cracker A), see Figure 11, the corresponding estimates for population of cracker A are $\hat{\rho}_1^2 = 0.9751$ and $\hat{\rho}_2^2 = 0.9747$; meanwhile estimates for population of cracker B are, $\hat{\rho}_1^2 = 0.9714$ and $\hat{\rho}_2^2 = 0.9710$. Then we compute the probability that an extreme correlation structure as $r_1^2 = 0.9751$ and $r_2^2 = 0.9747$ due to population correlation structure estimates of cracker A with the given template, occurs under the distribution of the correlation structure influenced by the template and population of cracker B. After integration of distribution of Theorem 3.1 we have that $P((r_1^2, r_2^2) > (0.9751, 0.9747)) < 0.0017$, which means that the Eulerian shape of cracker A is so far from the Eulerian shape of cracker B. Figure 12 shows the associated distribution of the template and an approximate region for integration.

METHOD 3: USING A TEMPLATE CLOSE TO CRACKER B:

If we select a template where 4 of the 5 coincident landmarks of method 1, are place on the sides of the rectangle (more closer to cracker B), see Figure 13 the corresponding estimates for population of cracker A are $\hat{\rho}_1^2 = 0.8928$ and $\hat{\rho}_2^2 = 0.8927$; meanwhile estimates for population of cracker A are, $\hat{\rho}_1^2 = 0.9569$ and $\hat{\rho}_2^2 = 0.9567$. Then we compute the probability that an extreme correlation structure as $r_1^2 = 0.9569$ and $r_2^2 = 0.9567$ due to population correlation structure estimates of cracker b with the given template, occurs under the distribution of the correlation structure influenced by the template and population of cracker A. After integration of distribution of Theorem 3.1 we have that $P((r_1^2, r_2^2) > (0.9569, 0.9567)) < 0.00038$, which means that the Eulerian shape of cracker A is so far from the Eulerian shape of cracker B. Figure 14 shows the associated distribution of the

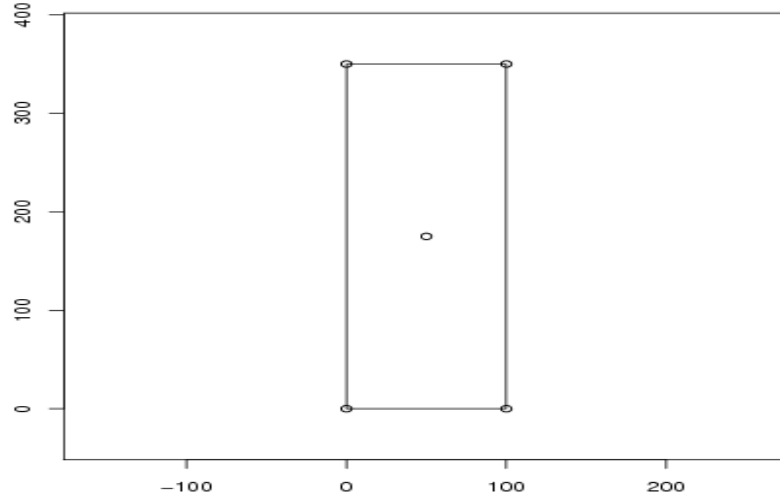


Figure 9: A degenerated template

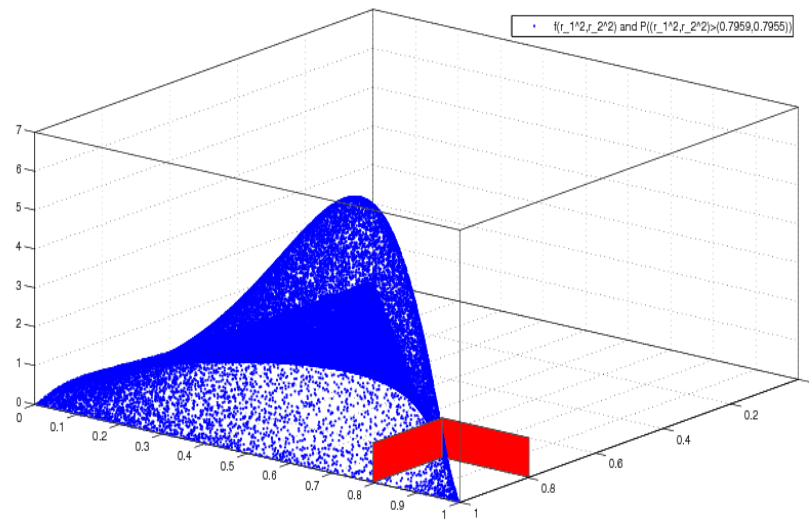


Figure 10: Eulerian polynomial joint distribution of a degenerated template vs cracker B and a test for a cracker A.

template and an approximate region for integration.

Note that the three methods ratifies the same conclusion about Eulerian shape difference, which seems to be independent on the template (of course it must satisfies the geometrical invariants demanding for Eulerian shape). In some experiments is difficult to suggest a template, but the

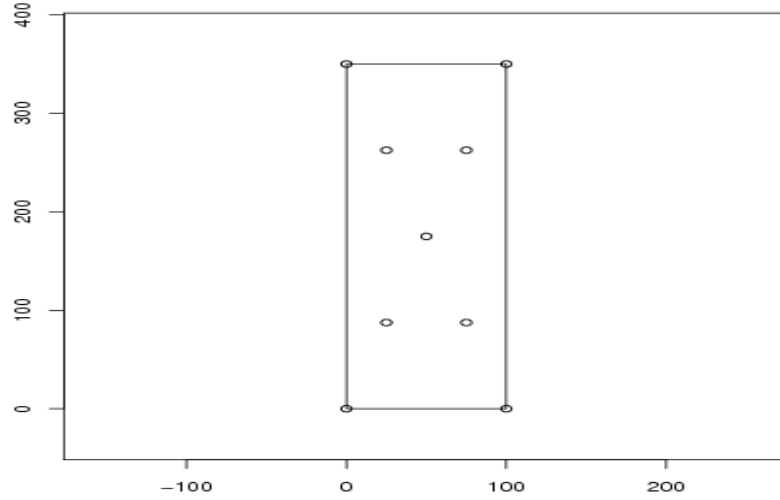


Figure 11: A template close to cracker A.

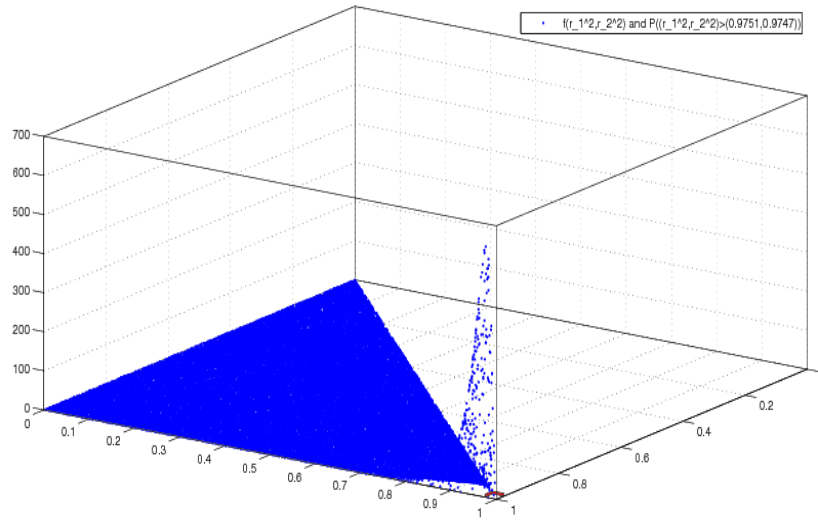


Figure 12: Eulerian polynomial joint distribution of a cracker B and template similar to cracker A, and a test for cracker A.

addressed Heuristic independence shows that it is not a matter of big difference among the two pairs of estimates, but the joint distribution tends to be so narrow when the estimates are close as in method 2, meanwhile a degenerated template will provide apart enough the pairs of estimates but the joint distribution for testing is so wide, as we can see in method 3. Medium difference as

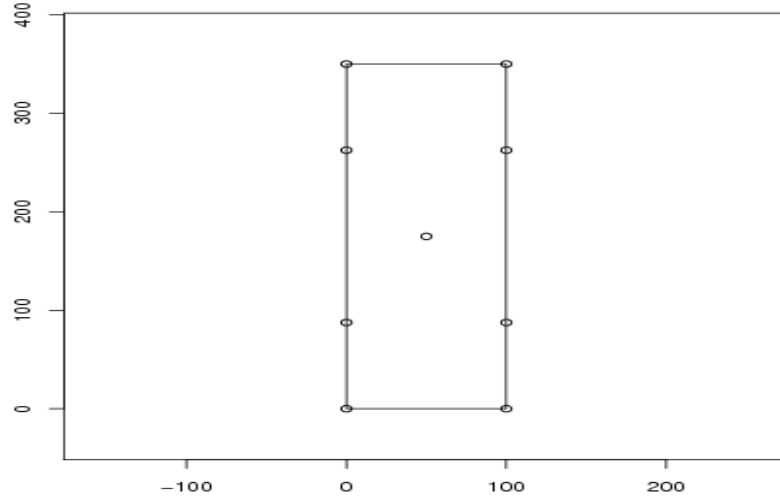


Figure 13: A template close to cracker B.

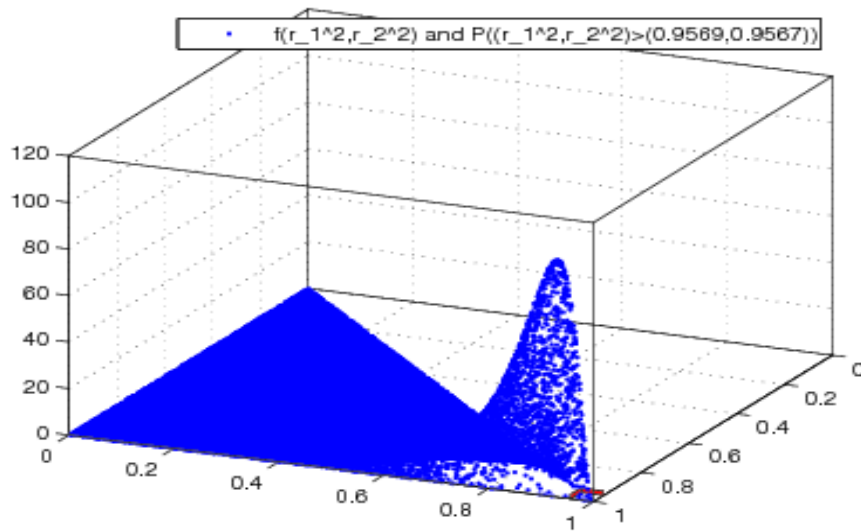


Figure 14: Eulerian polynomial joint distribution of a cracker A and a template similar to cracker B, and a test for cracker B.

in method 1 has a proportional joint distribution size. The most important fact is that in presence of shape differences, the selected template emerges as a theoretical or artificial object to perform the test, but it is irrelevant (in the sense of Eulerian restrictions). A very far artificial template will separate differences but the associated distribution has big variance, and it affects the resolution

of the test. Some mixing ideas for an artificial template close to intuition could be a good choice. Another usual conjecture for the template is a real observation of the sample, however, we have to be sure that the assigned template really belongs to the addressed population.

We try to apply this methodology with a very sensitive landmark data, the schizophrenia landmark data due to Bookstein (1996). In this case 13 landmarks in 2 dimensions, were register on a near midsagittal brain scan of 14 controls and 14 patients with schizophrenia. The landmarks chosen in the MRI were: (1) splenium, posteriormost point on corpus callosum; (2) genu, anteriormost point on corpus callosum; (3) top of corpus callosum, uppermost point on arch of callosum (all three to an approximate registration on the diameter of the callosum); (4) top of head, a point relaxed from a standard landmark along the apparent margin of the dura; (5) tentorium of cerebellum at dura; (6) top of cerebellum; (7) tip of fourth ventricle; (8) bottom of cerebellum; (9) top of pons, anterior margin; (10) bottom of pons, anterior margin; (11) optic chiasm; (12) frontal pole, extension of a line from landmark 1 through landmark 2 until it intersects the dura; (13) superior colliculus; see Bookstein (1996) and Dryden and Mardia (1998).

First we use as a template one of the MRI sampled from schizophrenic patients, see Figure 15. The computations are simpler and no new integrals must be computed in Theorem 3.1, because this data base has the same number of landmarks than the previously studied problem of handwritten digit 3. Again the distribution of the squared canonical correlation population is just a polynomial of degree 12 in the latent roots of the matrix argument.

The corresponding estimates for population of schizophrenic patients are $\hat{\rho}_1^2 = 0.9790$ and $\hat{\rho}_2^2 = 0.9789$; meanwhile estimates for population of controls are a little less as we expect, $\hat{\rho}_1^2 = 0.9783$ and $\hat{\rho}_2^2 = 0.9781$. Then we compute the probability that an extreme correlation structure as $r_1^2 = 0.9790$ and $r_2^2 = 0.9789$ due to population correlation structure estimates of schizophrenic patients with the given template, occurs under the distribution of the correlation structure influenced by the template and population of controls. After integration of distribution of Theorem 3.1 we have that $P((r_1^2, r_2^2) > (0.9790, 0.9789)) < 0.0024$, which means that the Eulerian shape of schizophrenic patients is different from the Eulerian shape of controls. Figure 16 shows the associated distribution of the template and an approximate region for integration.

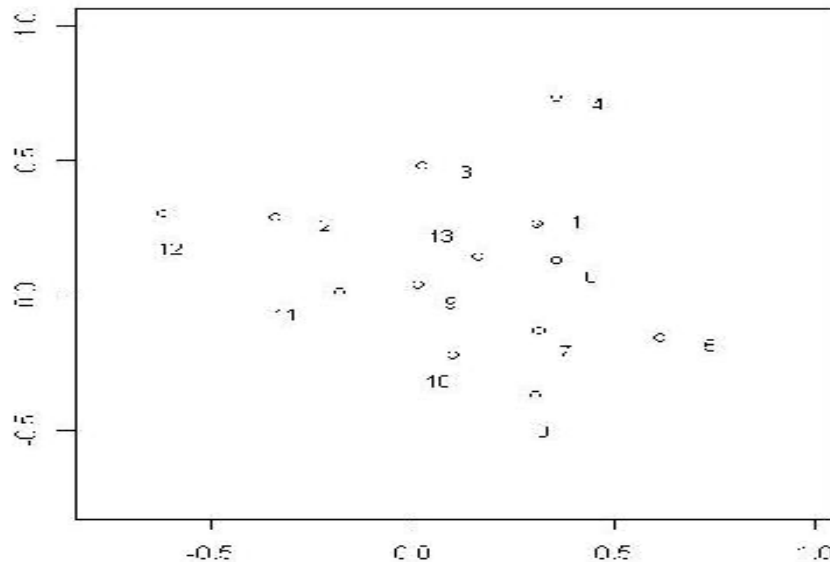


Figure 15: A template corresponding to a randomly sampled schizophrenic patient.

A similar result is obtained by taking an arbitrary template randomly selected from the sample of controls.

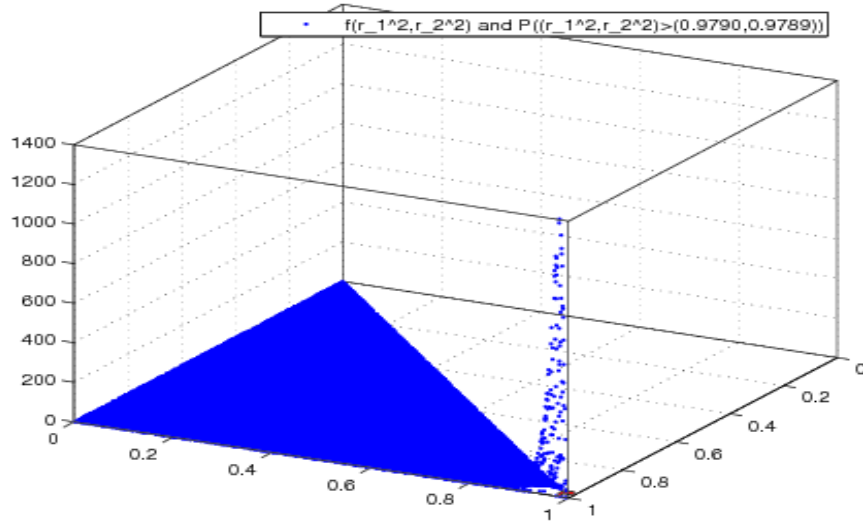


Figure 16: Eulerian polynomial joint distribution of controls and a schizophrenic patient-template, and a test for schizophrenic patients.

Concluding remark: Finally, observe that the exact Eulerian polynomial joint distribution can be used for testing the structure of correlation, as in the same way that equality mean shape tests are usually done in shape analysis, with the difference that we are using the exact distribution instead of the asymptotic distributions of the statistics traditional implemented. Of course, the inference on correlation structure differs from the inference about mean shape, and both analysis complement each other, but it seems that the Eulerian shape analysis is sufficient for detecting differences between populations as the similar mean shape analysis. In fact, we have applied the methods presented here to some of the classical landmark data studied in literature by asymptotic distributions or inference in the tangent plane as those presented in Dryden and Mardia (1998), and we have obtained the same conclusions about mean shape differences, among the applications we do not include in this manuscript we count the following landmark data: mouse vertebra, gorilla skulls and macaque skulls. However, for completeness, a subsequent work will include the addressed associated Eulerian mean shape theory and we will back to this applications.

Observe, that the exact Eulerian polynomial joint distribution can be used for testing the structure of correlation, as in the same way that equality mean shape tests are usually done in shape analysis, with the difference that we are using the exact distribution instead of the asymptotic distributions of the statistics traditional implemented. Of course, the inference on correlation structure differs from the inference about mean shape, and both analysis complement each other. In fact, a subsequent work will include the addressed associated Eulerian mean shape theory and we will back to this applications.

Acknowledgments

F. Caro was supported by University of Medelln in the context of a join research project with University of Toulouse and University of Bordeaux.

References

- Bookstein, F. L. (1996). Biometrics, biomathematics and the morphometric synthesis. *Bulletin of Mathematical Biology*, 58, 313-365.
- Caro-Lopera, F. J. (2014). Generalized Mellin transform and families of matrix-variate polynomial distributions. *Submitted*.
- Caro-Lopera, F. J., Díaz-García, J. A., González-Farías, G. (2014c). Inference in affine shape theory under elliptical models. *Journal of the Korean Statistical Society*, 43:67-77.
- Caro-Lopera, F. J., González-Farías, G., Balakrishnan, N. (2013a). Determinants, permanents and some applications to statistical shape theory. *Journal of Multivariate Analysis*, 114:29-39.
- Caro-Lopera, F. J., Díaz-García, J. A. and González-Farías, G. (2006). A Formula for Complex Zonal Polynomials of Second Order. *Revista de Matemática: Teoría y Aplicaciones*, 13(1), 35–39.
- Caro-Lopera, F. J., Díaz-García, J. A. and González-Farías, G. (2007). A formula for Jack polynomials of the second order. *Aplicaciones Mathematicae*, 34, 113-119.
- Caro-Lopera, F. J., Díaz-García, J. A., & González-Farías, G. (2009b). Inference in statistical shape theory: Elliptical configuration densities. *Journal of Statistical Research*, 43(1), 1-19.
- Caro-Lopera, F. J., Díaz-García, J.A., González-Farías, G. (2010). Noncentral elliptical configuration density. *Journal of Multivariate Analysis*, 101:32-43.
- Caro-Lopera, F. J., González-Farías, G., and Balakrishnan, N. (2014). On Generalized Wishart Distributions - I: Likelihood Ratio Test for Homogeneity of Covariance Matrices. *Sankhyā A*, 76-A(2):179-194.
- Caro-Lopera, F. J., González-Farías, G., and Balakrishnan, N. (2014). On generalized Wishart distribution - II: Sphericity test. *Sankhyā A*, 76-A(2):195-218.
- Constantine, A. C. (1963). Noncentral distribution problems in multivariate analysis. *Annals of Mathematical of Statistics*, 34, 1270-1285.
- Davis, A. W. (1979). Invariant Polynomials with two Matrix Arguments Extending the Zonal Polynomials: applications to Multivariate distribution theory. *Annals of the Institute of Statistical Mathematics*, 31, 465-485.
- Davis, A. W. (1980). Invariant polynomials with two matrix arguments, extending the zonal polynomials. *Multivariate analysis, V* (P.R. Krishnaiah, Ed.), pp. 287–299, North-Holland, Amsterdam-New York, 1980.
- Díaz-García, J.A. & Caro-Lopera, F.J. (2010). Shape theory via affine transformation: Some generalisations. Cornell University Library. arXiv:1012.5856. Also submitted.
- Díaz-García, J.A. & Caro-Lopera, F.J. (2012a). Statistical theory of shape under elliptical models and singular value decompositions. *Journal of Multivariate Analysis*, 103, 77-92.
- Díaz-García, J.A., Caro-Lopera, F.J. (2012b). Generalised shape theory via SV decomposition. *Metrika*, 75, 541-565.
- Díaz-García, J.A., Caro-Lopera, F.J. (2014). Statistical theory of shape under elliptical models via QR decomposition. *Statistics*, 48, 456-472.
- Díaz-García, J. A., & Caro-Lopera, F. J. (2016). Statistical theory of shape under elliptical models via polar decompositions. *Utilitas Mathematica*. Accepted for publication.
- Díaz-García, J. A., & Caro-Lopera, F. J. (2015). Matrix generalised Kummer relation. *South African Statistical Journal*, Volume 49 (1), in press.

- Díaz-García, J. A., & Caro-Lopera, F. J. (2008). About test criteria in multivariate analysis. *Brazilian Journal of Probability and Statistics*, 22(1), 35–59.
- Díaz-García, J. A., Gutiérrez, J. R., & Ramos-Quiroga, R. (2003). Size-and-shape cone, shape disk and configuration densities for the elliptical models. *Brazilian Journal of Probability and Statistics*, 17, 135–146.
- Domokos, C., & Kato, Z. (2010). Parametric estimation of affine deformations of planar shapes. *Pattern Recognition*, 43, 569 – 578.
- Dryden I. L., & Mardia, K. V. (1998). *Statistical shape analysis*. John Wiley and Sons, Chichester.
- Ecabberth, O., & Thiran, J.(2004). Adaptive Hough transform for the detection of natural shapes under weak affine transformations. *Pattern Recognition Letters* 25, 1411–1419.
- Glasbey, C. A., & Mardia, K. V. (2001). A penalized likelihood approach to image warping. *Journal of the Royal Statistical Society: Series B*, 63, Part 3, 465–514.
- Goodall, C. (1991). Procrustes methods in the statistical analysis of shape (with discussion). *Journal of the Royal Statistical Society: Series B*, 53, 285-339.
- Goodall, C. R., & Mardia, K. V. (1993). Multivariate aspects of shape theory. *Annals of Statistics*, 21, 848–866.
- Groisser, D., & Tagare, H. (2009). On the Topology and Geometry of Spaces of Affine Shapes. *Journal of Mathematical Imaging and Vision*, 34, 222-233.
- Herz, C. S. (1955). Bessel functions of matrix argument. *Annals of Mathematics*, 61, 474–523.
- Horgan, G. W., Creasey, A. & Fenton, B. (1992). Superimposing two dimensional gels to study genetic variation in malaria parasites. *Electrophoresis*, 13, 871–875.
- James, A. T. (1964). Distributions of matrix variate and latent roots derived from normal samples, *Annals of Mathematical of Statistics*, 35 (1964) 475–501.
- James, A. T. (1968). Calculation of zonal polynomial coefficients by use of the Laplace-Beltrami operator. *The Annals of Mathematical Statistics*, 39, 1711–1718.
- Kendall, D. G., Barden, D., Carne, T. K. & Le, H. (1999). *Shape and Shape theory*. John Wiley & Sons Ltd., Chichester.
- Kent, J. T., Mardia, K. V. & Taylor, C. C. (2004). Matching problems for unlabelled configurations. Proceedings in Bioinformatics, *Images and Wavelets*. 33–36. Edited by Aykroyd, R.G., Barber, S. and Mardia, K.V. Leeds, Leeds University Press.
- Koev P., & Edelman, A. (2006). The efficient evaluation of the hypergeometric function of a matrix argument. *Mathematics of Computation*, 75, 833–846.
- Leung, T., Burl, M. & Perona, P. (1998). Probabilistic Affine Invariants for Recognition, *Proceedings Conf. Computer Vision and Pattern Recognition*, June, Santa Barbara, California.
- Lin, W. S. & Fang, C. H. (2007). Synthesized affine invariant function for 2D shape recognition. *Pattern Recognition*, 40, 1921– 1928
- Lindeberg, T., & Garding, J. (1997). Shape-adapted smoothing in estimation of 3-D shape cues from affine deformations of local 2-D brightness structure. *Image and Vision Computing*, 15, 415–434
- Mai, F., Chang, C. Q., & Hung, Y. S. (2011). A subspace approach for matching 2D shapes under affine distortions. *Pattern Recognition*, 44, 210–221.

- Mardia, K. V. & Patrangenaru, V. (2005). Directions and projective shapes. *The Annals of Statistics*, 33 (4), 1666–1699
- Mardia, K. V., Goodall, C. & Walder, A. (1996). Distributions of projective invariants and model-based machine vision. *Advances in Applied Probability*, 28, 641–661.
- Mardia, K. V., Patrangenaru, V. & Sugathadasa, S. (2005). Protein Gels Matching. In *Quantitative Biology, Shape Analysis, and Wavelets*. (Barber, S., Baxter, P. D., Mardia, K. V. & Walls, R. E. (Eds.)). 163-165. Leeds, Leeds University Press.
- Mokhtarian, F., & Abbasi, S. (2002). Shape similarity retrieval under affine transforms. *Pattern Recognition*, 35, 31–41.
- Muirhead, R. J. (1982). *Aspects of multivariate statistical theory*. Wiley Series in Probability and Mathematical Statistics. John Wiley & Sons, Inc. New York.
- Patrangenaru, V. & Mardia, K.V. (2003). Affine Shape Analysis and Image Analysis. *Proceedings in Stochastic Geometry, Biological Structure and Images*, 57–62. Edited by Aykroyd, R. G., Mardia, K. V. & Langdon, M.J. Leeds, Leeds University Press.
- Raftery, A. E. (1995). Bayesian model selection in social research. *Sociological Methodology*, 25, 111–163.
- Sawyer, P. (1997). Spherical Functions on Symmetric Cones. *Transactions of the American Mathematical Society*, 349, 3569–3584.
- Small, C. G. (1996). *The Statistical Theory of Shape*. Springer, New York.